Available online at www.sciencedirect.com
SCIENCE DIRECT®
Clinical Biomechanics 21 (2006) 107–115
CLINICAL BIOMECHANICS
www.elsevier.com/locate/clinbiomech

Effect of handrim diameter on manual wheelchair propulsion: Mechanical energy and power flow analysis

Lan-Yuen Guo [a,b], Fong-Chin Su [a,*], Kai-Nan An [c]

[a] Institute of Biomedical Engineering, National Cheng Kung University, Motion Analysis Laboratory, 1 University Road, Tainan 701, Taiwan
[b] Faculty of Sports Medicine, Kaohsiung Medical University, Kaohsiung, Taiwan
[c] Biomechanics Laboratory, Division of Orthopedic Research, Mayo Clinic, Rochester, MN, USA

Received 17 October 2002; accepted 22 August 2005

Abstract

Background. Wheelchair design parameters such as handrim diameter could affect propulsion. The purpose of this study was to examine the effect of handrim size (0.54, 0.43, and 0.32 m) on mechanical energy and power flow during wheelchair propulsion.

Methods. Twelve young normal male adults (mean age 23.5 years old) were recruited in this study. Both 3-D kinematic and kinetic data of the upper extremity were collected synchronously using a Hi-Res Expert Vision motion system and an instrumented wheel during wheelchair propulsion.

Findings. The kinetic, potential and total mechanical energy of the upper extremity increased as the handrim size increased. For each upper arm segment, the joint translational power and the rotational power of the proximal joint increased with increasing handrim size. The work done during a complete propulsion cycle with the larger handrim size is significantly larger than that using a smaller handrim ($P < 0.05$).

Interpretation. The increased kinetic, potential and total mechanical energy were due to the increased linear velocity and the elevated positions of the upper extremity segments. The shoulder and trunk flexors increased the magnitude of their concentric contractions during propulsion with the large handrim as increased output power is required. By using mechanical energy and power flow analysis techniques, we evaluated the previously-reported effect of handrim size on mechanical cost and provided insight into the relationship between the two.

Keywords: Wheelchair; Handrim size; Mechanical energy; Power flow

1. Introduction

Many factors can affect performance during manual wheelchair propulsion. These include seat height (Van Der Woude et al., 1989; Masse et al., 1992; Hughes et al., 1992; Wei et al., 2003), fore-aft axle position (Masse et al., 1992; Hughes et al., 1992; Wei et al., 2003), handrim diameter (Van Der Woude et al., 1988), handrim tube diameter (Van Der Linden et al., 1996), wheelchair design (Rudins et al., 1997; Davis et al., 1998) and wheelchair weight (Bednarczyk and Sanderson, 1995; Ruggles et al., 1994). In the literature available, the influence of variation in designs upon cardio-respiratory factors (Van Der Woude et al., 1989, 1988), energy cost (Van Der Woude et al., 1989, 1988), kinematics, kinetics (Ruggles et al., 1994; Veeger et al., 1992b) and electromyography (EMG) (Masse et al., 1992; Veeger et al., 1989; Mulroy et al., 2004) have been examined. Most investigations have focused on physiological (Van Der Woude et al., 1989, 1988) and movement parameters; few have investigated kinetic changes (Ruggles et al., 1994) between the different

* Corresponding author.
E-mail address: fcsu@mail.ncku.edu.tw (F.-C. Su).

0268-0033/$ - see front matter © 2005 Elsevier Ltd. All rights reserved.
doi:10.1016/j.clinbiomech.2005.08.015

designs. Bednarczyk and Sanderson (1995) found no effect of wheelchair weight on the kinematics of wheelchair propulsion and felt the effect would be more appropriately revealed using kinetic measures (Bednarczyk and Sanderson, 1995).

Lately, several groups have been working on the development of kinetic models of manual wheelchair propulsion (Asato et al., 1993; Cooper et al., 1997; Wu et al., 1998; Boninger et al., 1997; Veeger et al., 1992b; Robertson et al., 1996; Veeger and Van Der Woude, 1991; Sabick et al., 2004; Van Drongelen et al., 2005). However, thus far, only net joint force or net moments have been calculated for the wrist, elbow and shoulder joints. A net joint moment represents the internal response of a body segment to an external load. All of these models are not sufficient to fully explain the low efficiency of manual wheelchair propulsion and the high incidence of upper extremity complaints.

The effect of handrim size was investigated by Van Der Woude et al. (1988). They examined the effects of handrim diameter (0.30, 0.35, 0.38, 0.47, and 0.56 m) on physiological and movement parameters. They found that propelling with a smaller handrim had a lower metabolic cost and higher systematic mechanical efficiency and concluded this may due to the decreased segmental excursions of the upper extremity and lower linear hand velocity. Metabolic cost was quantified by oxygen consumption and heart rate measures. However, they offered limited insight into the causes of efficiency differences in terms of net moment and force.

To our knowledge, most mechanical models of wheelchair propulsion used to investigate mechanical inefficiencies in the movement have focused on the concept of fraction effective force (Dallmeijer et al., 1998; Veeger et al., 1992a,b; De Groot et al., 2003; Morrow et al., 2003; Boninger et al., 2002; De Groot et al., 2002), some studies revealed during propulsion almost 50% of the forces exerted at the pushrim are not directed toward forward motion and, therefore, either are applied friction to the pushrim or are wasted. Some investigators do not agree with the concept that non-tangentially directed forces are wasted or just misdirected, but effective regarding co-ordination and physiology (Veeger et al., 1991; Rozendaal et al., 2003; De Groot et al., 2002).

Few have used mechanical energy and power flow analysis for this purpose (Guo et al., 2003; Van Der Helm and Veeger, 1999). We used mechanical energy and power flow calculations to understand the characteristics of wheelchair propulsion and examine the effect of handrim size. In this study, the effects of handrim diameter (0.54, 0.43, and 0.32 m) on mechanical energy and power flow were quantified. Our assumption is that the smaller the handrim size, the less mechanical work is required to propel the wheelchair. Our study examined if these two measures (mechanical energy and power flow) could support this assumption. Furthermore, we aimed to determine if these measures could give us more insight into the metabolic differences between propulsion with different handrim sizes.

2. Method

Twelve young normal male adults (mean age 23.5 years), without any reported upper extremity disorder, were included in this study. The ExpertVision™ system (Motion Analysis Corp., Santa Rosa, CA, USA) was used to record the trajectories (at 60 Hz) of 15 reflective markers placed unilaterally on selected anatomic landmarks on each subject. The anatomic landmarks were as follows: processes xiphoideus, sternal notch, spinous process of the 7th cervical vertebra, acromion process, medial and lateral epicondyles of the elbow, radial and ulnar styloid processes, 3rd metacarpal, knuckle II and knuckle V. In addition, a triangular frame with three-markers was placed on the upper arm (Wu et al., 1998). An instrumented wheel system was used to directly measure three-dimensional dynamic forces and moments on the handrim during wheelchair propulsion in a laboratory setting (Wu et al., 1998).

Three handrim diameters, 0.54, 0.43, and 0.32 m, were assigned to each subject in a randomized order. They were characterized as large, middle and small, respectively. Each subject had to propel for at least five propulsion cycles for each handrim size. Each variable was averaged for these five trials to represent the subject's performance for the given handrim size. Also, these averaged variables for each subject were averaged again for all subjects to represent the ensemble performance for a given handrim size. The markers' positions were used to define the coordinate system for each segment and Euler angles and Euler parameters were determined to represent the joint and segmental kinematics of the upper extremity. The measured forces and moments on the handrim were used to determine the kinetics, joint forces and moments, of the upper extremity using an inverse dynamic method (Wu et al., 1998; Guo et al., 2003). These parameters were used for further calculation of mechanical energy and power flow.

The total mechanical energy (E) of a segment is the sum of its potential (E_p) and kinetic energies (E_k).

$$E = E_p + E_k = mgh + \frac{1}{2}mv^2 + \frac{1}{2}I\omega^2$$

where $v = \sqrt{v_x^2 + v_y^2 + v_z^2}$, m is the segment mass, g is gravitational force, h is the height of the segment, v is the magnitude of the velocity of the segment, I is the moments of inertia corresponding to the principal inertia axes of the segment and ω is the angular velocity of the segment. The magnitude of the velocity is derived from all three components (v_x, v_y, v_z) of the velocity of the segment's center of mass in the global coordinate

system. The rate of change of the mechanical energy was calculated to determine the *mechanical power* (P_m) requirements of the segment during wheelchair propulsion.

$$P_m = \frac{dE}{dt}$$

The power requirements of the segments discussed above are derived from the segmental mechanical energy calculations. These requirements were compared with the power input into and transferred from the joints as calculated from the resultant joint loads and the segmental velocities.

The joint power ($\boldsymbol{P}_j$) is equal to the vector dot product of the net joint force ($\boldsymbol{F}$) and the joint translational velocity ($\boldsymbol{V}$). The muscle power ($\boldsymbol{P}_m$) is the net joint moment ($\boldsymbol{M}$) dotted with the segmental angular velocity (ω) (not the joint rotational velocity) (Fig. 1a). Note that the forces and moments must be expressed in the same coordinate system as the segment velocity. The power flow of a segment was composed of the proximal/distal joint power ($\boldsymbol{P}_{jp}$ and $\boldsymbol{P}_{jd}$, distal denoted d, proximal p) and proximal/distal muscle power ($\boldsymbol{P}_{mp}$ and $\boldsymbol{P}_{md}$) (Fig. 1b). The total power flow applied to or taken from the body is the summation of the joint power and muscle power at each end. For a typical segment, the equation expressing the joint muscle and total power is

$$\begin{aligned}\boldsymbol{P}_j &= \boldsymbol{F}\cdot\boldsymbol{V}\\ \boldsymbol{P}_m &= \boldsymbol{M}_p\cdot\boldsymbol{\omega}\\ \boldsymbol{P}_f &= \boldsymbol{P}_{jp}+\boldsymbol{P}_{mp}+\boldsymbol{P}_{jd}+\boldsymbol{P}_{md}\\ &= \boldsymbol{F}_p\cdot\boldsymbol{V}_p+\boldsymbol{M}_p\cdot\boldsymbol{\omega}+\boldsymbol{F}_d\cdot\boldsymbol{V}_d+\boldsymbol{M}_d\cdot\boldsymbol{\omega}\end{aligned}$$

Subscript d and p represent the distal and proximal ends of the segment respectively.

A relatively high correlation between work done by mechanical power and metabolic cost were found in past walking and running studies, even for normal subjects (Frost et al., 1997; Burdett et al., 1983). However, there have been no investigations into the relationship between metabolic cost and mechanical power during wheelchair propulsion. The work calculated from the mechanical power (W_m) and the power flow (W_p) for one propulsion cycle was determined by the following equation, which allows transfer of energy between adjacent segments of the same limb, but not between limbs and the trunk (Frost et al., 1997; Unnithan et al., 1999).

$$W_m = \sum_{j=1}^{N}\left|\sum_{i=1}^{S}\left(\frac{dE}{dt}\right)\right| = \sum_{J=1}^{N}\left|\sum_{i=1}^{S}P_m\right|$$

$$W_p = \sum_{j=1}^{N}\left|\sum_{i=1}^{S}P_f\right|$$

where N is the number of data points and S represents the total number of segments.

Variables were normalized to 100% propulsion cycle. Each propulsion cycle included propulsion and recovery phases. Therefore each variable could be averaged for these five trials to represent the subject's performance for each handrim size. In addition, the averaged variables for each subject were averaged again to represent the ensemble average for a given handrim size. A repeated measures ANOVA was used to test for differences between handrim sizes. Tukey's post-hoc test was used to determine the significance between each

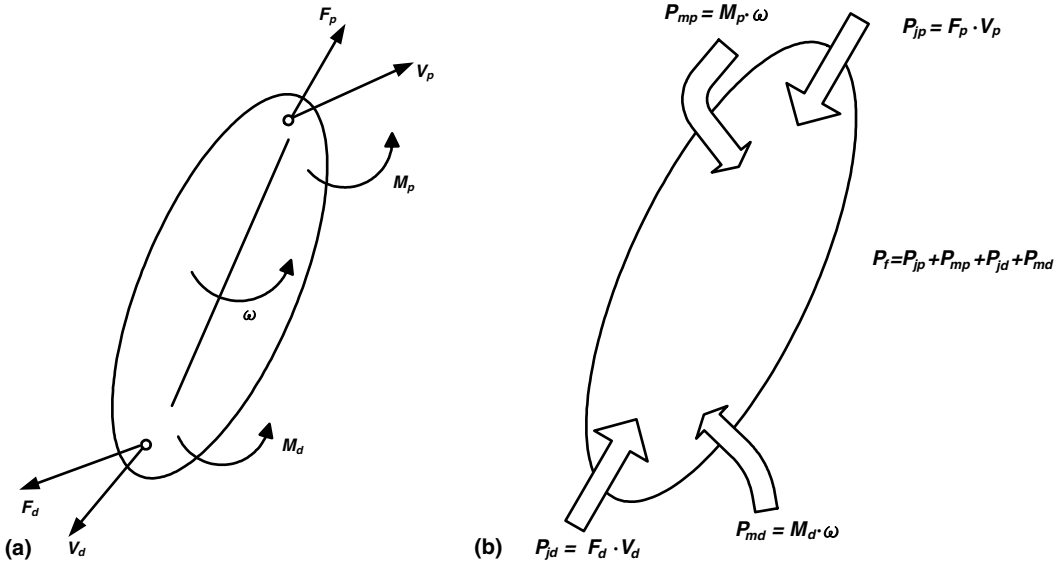

Fig. 1. (a) Variables included in the calculation of the joint power ($\boldsymbol{P}_j$) and muscle power ($\boldsymbol{P}_m$) for a rigid body, $\boldsymbol{P}_j = \boldsymbol{F}\cdot\boldsymbol{V}$, $\boldsymbol{P}_m = \boldsymbol{M}_p\cdot\boldsymbol{\omega}$. (b) Total power flow ($\boldsymbol{P}_f$) is composed by the summation of the joint and muscle power at proximal and distal ends (Subscript p and d meant the proximal and distal part of segment respectively). $\boldsymbol{P}_f = \boldsymbol{P}_{jp} + \boldsymbol{P}_{mp} + \boldsymbol{P}_{jd} + \boldsymbol{P}_{md}$.

pairing of conditions. The significance level was set at $P < 0.05$.

3. Results

A stick diagram representation of the upper extremity during wheelchair propulsion with different handrim sizes is shown in Fig. 2 with a 0.05 s interval between data points. The solid and dotted lines represent 0.32 and 0.54 m handrim diameters, respectively. The upper extremity segments always moved downward and forward during the propulsion phase and upward and backward during the recovery phase. The upper extremity segments had a greater movement excursion and greater linear velocity when propelling the large handrim than when propelling the small handrim. The positions of the upper extremity segments and joints when maneuvering the large handrim were higher than those propelling the small handrim.

The total mechanical energy of a segment is composed of its potential and kinetic energy. Ground level is assumed to be zero potential energy. A representative graph of the upper arm segment energy during the propulsion cycle is shown in Fig. 3. In fact, the three upper extremity segments were characterized by similar trends. Kinetic energy increased during initial propulsion and reached a peak value at terminal-propulsion. Potential energy decreased from initial propulsion and had its least value at the end of the propulsion phase. During the propulsion phase, kinetic energy was the source for an increased total mechanical energy. However, during the recovery phase, the total mechanical energy increased due to the potential energy component. Both kinetic and potential energy increased with increased handrim size. The total mechanical energy pattern of

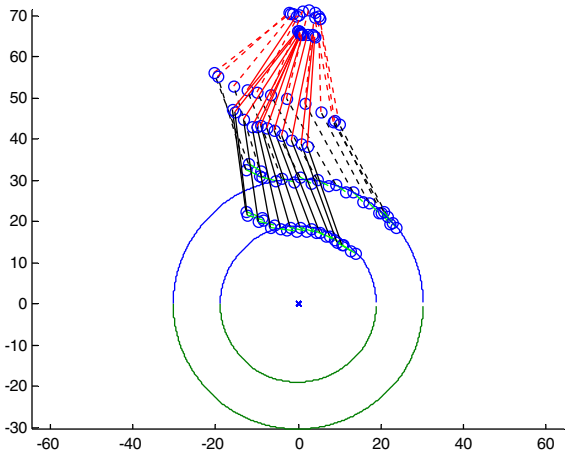

Fig. 2. Stick diagram representation of upper extremity for wheelchair propulsion during propulsion phase (solid line: 0.32 m; dot line: 0.54 m).

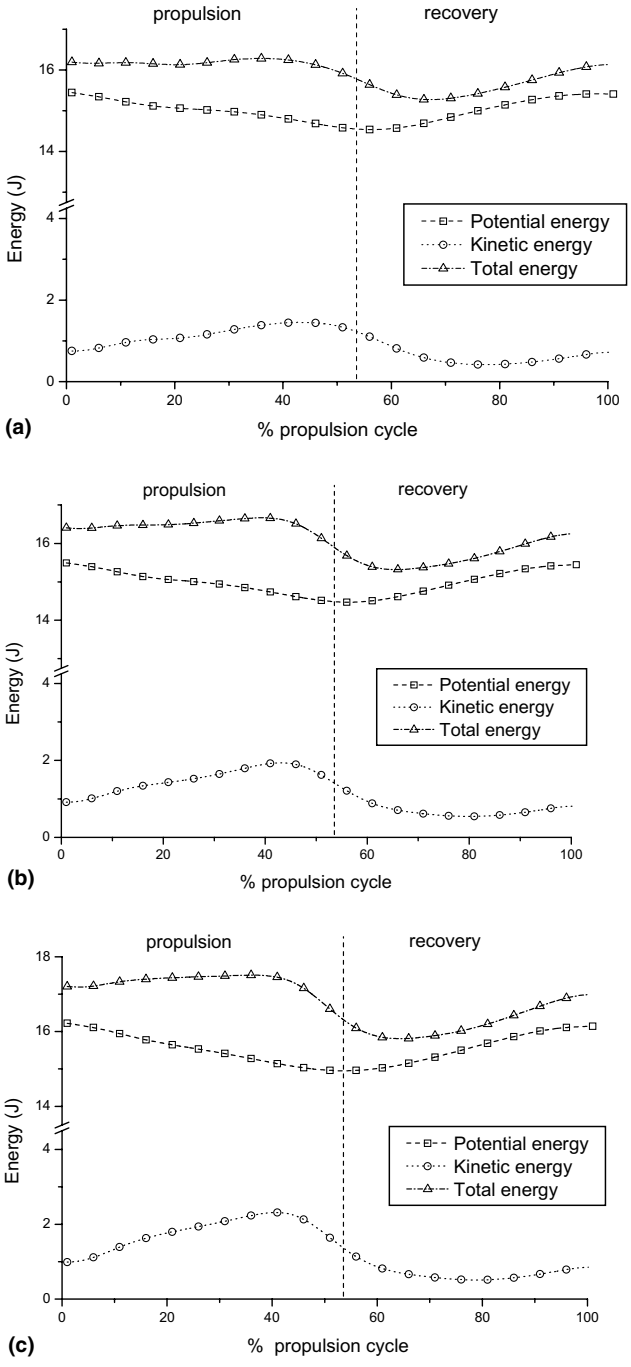

Fig. 3. Mean mechanical energy of the upper arm segment for different handrim sizes: (a) 0.32 m, (b) 0.43 m, and (c) 0.54 m.

the upper arm segment for the three handrim sizes are shown in Fig. 4(a). All three upper extremity segments showed similar trends during the propulsion cycle with their mechanical energy increasing from the initial propulsion until reaching its peak value at terminal propulsion. Then, the total mechanical energy decreased to its smallest value at initial recovery and then increased again until the end of the recovery phase. The total mechanical energy increased with increasing handrim

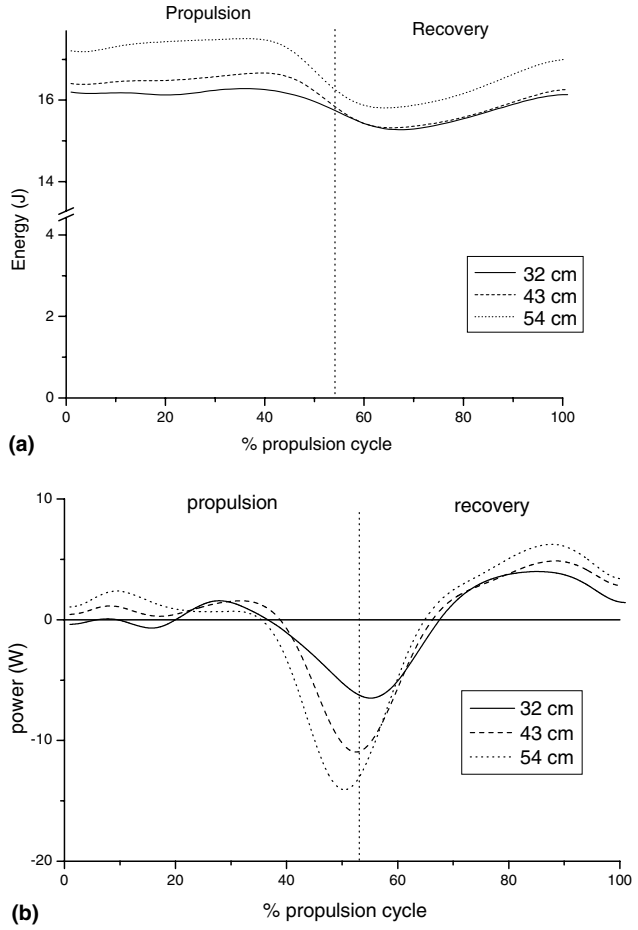

Fig. 4. Mean total mechanical energy (a) and rate of change of mechanical energy (b) of the upper arm segment for different handrim sizes.

size. The rate of change of total mechanical energy, mechanical power, of the upper arm segment is shown in Fig. 4(b). For the large handrim, the upper arm had greater positive power in initial propulsion and negative power in terminal propulsion.

Fig. 5 shows the components of power flow for the upper arm segment during propulsion for the different handrim sizes. The total power flow of a segment is composed of the joint translational power (P_J), muscle rotational power at the proximal and distal joints (P_M), and power due to the segment weights (P_W). The components of power flow showed that, with the exception of the upper arm, the active muscle rotational power components were small. In contrast, the joint translational power was quite large. During most of the propulsion phase, the proximal passive joint power is positive, i.e. energy flow into the segment, while the distal joint power is negative, i.e. energy flow out of the segment. In the upper arm segment, the magnitude of translational power at both the proximal and distal joints and rotational power at the proximal joint increased with increasing handrim size.

Total mechanical power and total power flow for all three upper extremity segments for the different handrim sizes are shown in Fig. 6. The patterns of mechanical power and power flow of all upper extremity segments were quite similar. The power is positive in the initial propulsion phase and negative in middle and terminal propulsion phases. The negative peak appeared near the end of the propulsion phase and then the power flow increased and reached a positive value in the mid-recovery phase. In general, the mechanical power and power flow showed similar trends. The positive power in initial propulsion phase and the negative power in terminal propulsion phase increased with increasing handrim size.

Work done during a complete propulsion cycle is listed in Table 1. The handrim size had a significant effect on both work calculated from the mechanical power (W_m) and from the power flow (W_p) ($P < 0.05$). The larger the handrim size, the greater the work done during a propulsion cycle. W_m was greatest for the 0.54 m handrim size, followed by the 0.43 m handrim, and was least in the 0.32 m handrim condition. Similarly, work calculated from power flow (W_p) was greatest for the 0.54 m handrim condition.

The external work produced by the wheelchair-user system per unit time during propulsion is expressed in terms of the dot product of the applied moment about the wheel axle and the angular velocity of the handrim. The mean external power during one propulsion cycle, with the three handrim sizes, is shown in Fig. 7. The external work, the integration of the external power, done to propel the 0.32, 0.43 and 0.54 m handrims, were 19.2 J (SD 5.5), 20 J (SD 6.6) and 21.2 J (SD 9.7), respectively. The F value is 0.83 and P value is 0.45 using a repeated measured ANOVA to test the statistical significance. There were no constraints on the external power in the experimental setting because each subject propelled the wheelchair at his chosen comfortable speed. Although the external work per propulsion cycle increased a little bit with increased handrim size, no statistically significant difference was found among the three handrim sizes.

4. Discussion

During the propulsion phase, the upper extremity and trunk musculature exert effort to propel the wheel forward so that the upper extremity segments are moved forward quickly. Therefore, the total mechanical energy during this phase increased, primarily due to increases in kinetic energy, especially the translational kinetic energy. Due to the movement constraint that the hand must follow the contour of the handrim during propulsion, the upper extremity segments have to move downward, causing the potential energy to

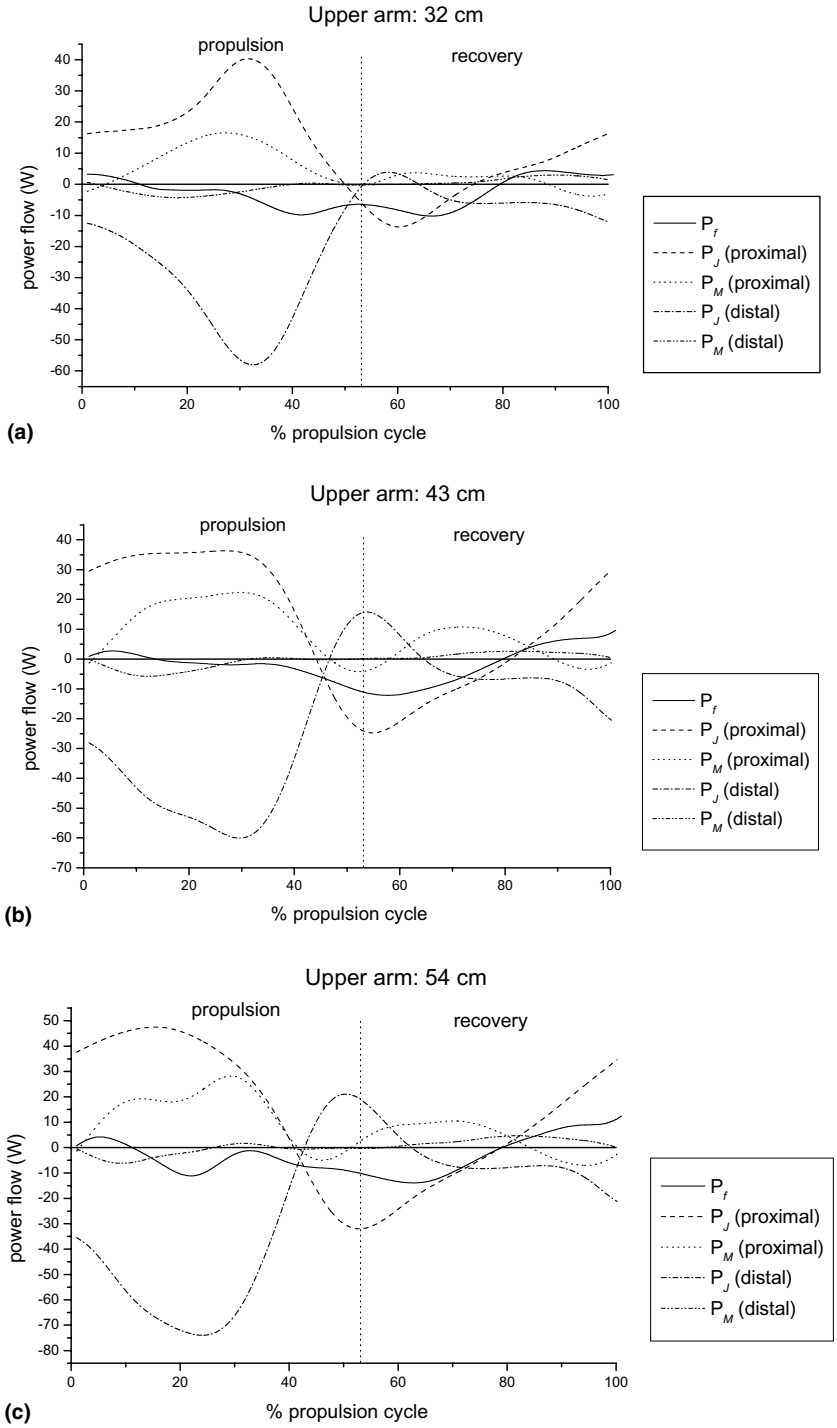

Fig. 5. Components of mean power flow of the upper arm segment for different handrim sizes: (a) 0.32 m, (b) 0.43 m, and (c) 0.54 m.

decrease. During the recovery phase, the upper extremity segments have to be repositioned on the handrim for the next propulsion. The segments move backward and upward slowly so the restoration of the total mechanical energy is mainly from potential energy. The mechanical energy pattern showed a complementary trend during most of the propulsion cycle, i.e. when kinetic energy increased, potential energy decreased over time. This complementary trend was not demonstrated in terminal propulsion phase, however, because the potential and kinetic energy decreased simultaneously. During terminal propulsion, the upper extremity segments are decelerated (for preparation of repositioning the hand) by eccentric muscle activity during the recovery phase, even

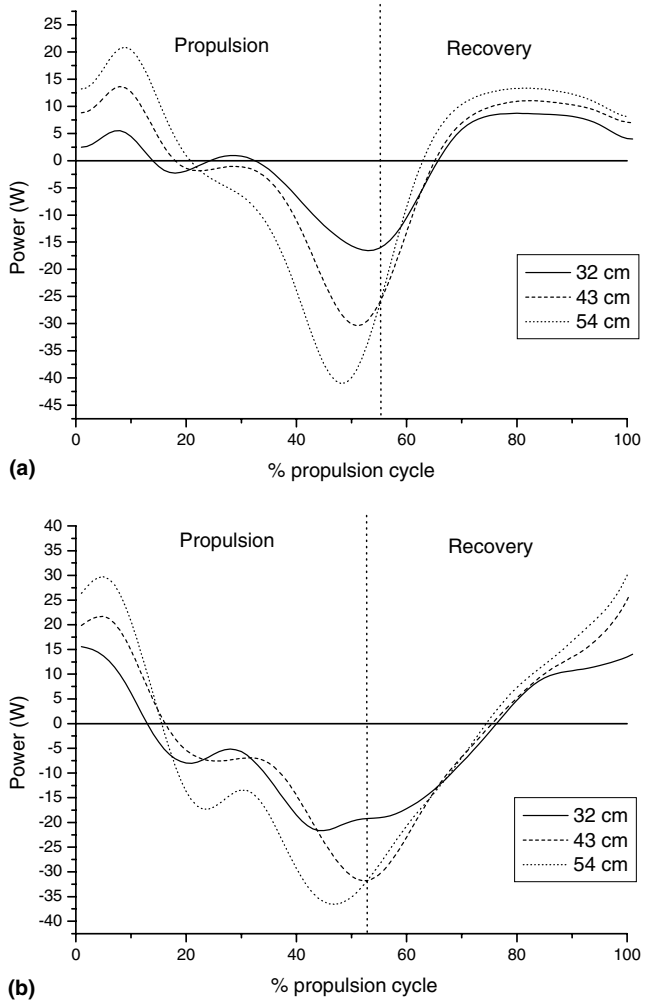

Fig. 6. Total mechanical power (a) and total power flow (b) for different handrim sizes.

Table 1
Work[a] calculated from mechanical power (W_m) and from power flow (W_p) for one propulsion cycle for each handrim size

	0.32 m	0.43 m	0.54 m	F value[b]	Post-hoc[c]
W_m	6.99 (2.41)	9.41 (2.50)	12.22 (4.02)	30.10*	0.54 m > 0.43 m > 0.32 m
W_p	11.68 (4.41)	13.70 (4.06)	16.47 (5.97)	10.06*	0.54 m > 0.43 m, 0.32 m

* $P < 0.001$.
[a] Means and SD in parenthesis, unit: J.
[b] Statistics was done with repeated measures ANOVA.
[c] Tukey's post-hoc test was used to determine the significance between each pair of the four groups.

though the segments are still moving downward and forward. This may be a potential explanation for the inefficiency of handrim wheelchair propulsion.

The total mechanical energy during wheelchair propulsion increased with increased handrim size (Fig. 4). Both the kinetic and potential energy increased as the handrim size increased. While propelling a larger handrim, the movement excursion increases but the propulsion time is not changed, so the linear velocity of the segments becomes higher and kinetic energy increases. The increase in potential energy is mainly caused by the higher positions of upper extremity segments in maneuvering a larger handrim. In the larger handrim, due to the greater linear velocity in initial propulsion phase, the rate of increase in kinetic energy is greater. Similarly, to stop the forward motion of the hand, which is moving at a high linear velocity before recovery phase, the rate of decrease in kinetic energy is larger for the larger handrim. Therefore, greater energy generation in initial propulsion and greater energy absorption in terminal propulsion are required to propel the larger handrim wheelchair.

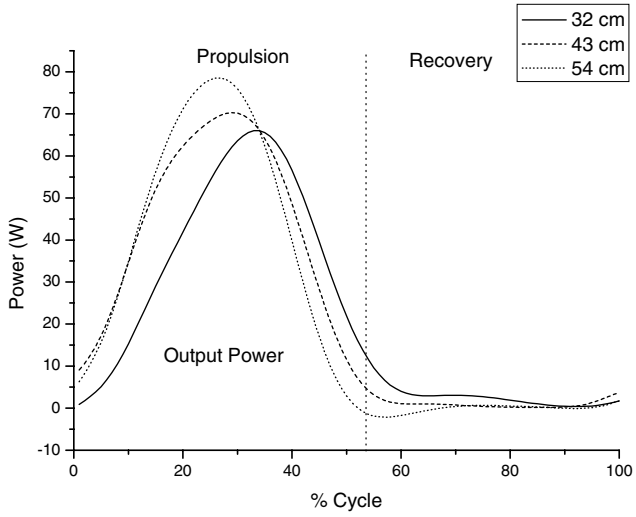

Fig. 7. The external power in propelling three different handrim sizes.

The energy change can be further elucidated by power flow analysis. Muscle power ($\boldsymbol{P}_m$), which is the net joint moment ($\boldsymbol{M}$) dotted with the segmental angular velocity (ω) (Fig. 5), is negative when the dominant muscles are eccentrically contracting. From past EMG studies (Masse et al., 1992; Veeger et al., 1989), we know which muscle group is dominant during the propulsion phase. During the propulsion phase, the increase in total mechanical energy is from both proximal muscular power and proximal joint power. However, the proximal joint power may be due to trunk flexors and proximal muscular power from the shoulder flexors. Trunk flexors concentrically contract to accelerate forward movement. At the same time, the shoulder flexor acts concentrically to speed up the shoulder flexion movement and generate a net joint angular power at the shoulder. These two powers are integrated and transferred to the forearm and hand to propel the wheel forward. Throughout the whole propulsion phase, the distal joint power of the hand was negative, i.e. indicating outflow. From

the terminal propulsion to middle recovery phase, the joint power flow is transferred upward to the trunk from the upper arm and forearm. This is to conserve the energy of the upper extremity in the trunk for the next propulsion cycle. During the initial recovery phase, the upper arm has proximal muscular power from the shoulder extensors. It acts concentrically to extend the shoulder and increases the potential energy of the upper arm segment. During late recovery phase, the total mechanical energy is increased by potential energy which is supplied by the proximal joint power, primarily from the trunk flexors. Concurrently, the trunk flexors eccentrically contract to slow down the backward movement of the trunk. This joint power again is transferred from the upper arm to the forearm and hand for the next propulsion cycle.

During the propulsion phase, the musculature in the upper extremity and trunk work to propel the wheel forward, especially the shoulder flexors and trunk flexors. The literature reveals that the largest joint moment appears at the shoulder (Robertson et al., 1996; Rodgers et al., 1998; Veeger and Van Der Woude, 1991; Su et al., 1993). In the upper arm segment, the magnitude of both proximal and distal joint power and proximal muscle power, increase with increasing handrim size. That implies that the shoulder flexors and trunk flexors increase their concentric contractions to propel the larger handrim. The power generated by these two major muscles groups will transfer distally to the forearm and hand providing the large output power required propelling a larger handrim. Therefore the increased effort of the shoulder flexors and trunk flexors are the source of increased joint power in the upper extremity. And the increased joint powers implicitly indicate increased joint forces and linear velocities of the joint centers. The muscle power acting on the forearm segment is much smaller than that acting on the proximal end of the upper arm. Two factors may be responsible for this phenomenon: (1) the elbow extensor moment is smaller than the shoulder flexor moment, and (2) the rotational velocity of the forearm is smaller than that of the upper arm. This phenomenon can be seen in the stick diagram (Fig. 2), i.e. the orientation of the forearm is more parallel in its sequential postures compared to the upper arm during the propulsion phase.

The assumption in this study is that propelling the wheelchair with the larger handrim size will have a greater metabolic cost. The results support this assumption; the required work to propel the larger handrim size is significantly larger than that using a smaller handrim. Our results concur with the study by Van Der Woude et al. (1988). They concluded that the larger handrim has a greater metabolic cost and their reasoning is that it may due to the increased segmental excursions of the upper extremity and higher linear hand velocity. In this study, we also found that the high linear velocities of the forearm, upper arm and hand caused an increased mechanical power. And using power flow analysis, we found that the joint forces and joint moments, which are determined by muscle contraction, also influence metabolic cost. Using mechanical energy and power flow analysis, we can evaluate the previously reported effect of handrim size on mechanical cost and provide insight into possible explanations.

Theoretically, the calculation of the rate of change of segmental total mechanical energy is equal to the sum of the segmental muscle and joint power. However, errors in the modeling of the human form and experimental error in the measuring equipment could produce discrepancies (Winter, 1994; Gordon et al., 1980). Since similar trends exist between the two different power calculations, our energetic model seems reasonable. A limitation of this study is that young normal male adults were included as subjects; experienced wheelchair users may have different energy and power flows. Also, it is possible to have co-contraction of muscles in the upper extremity during wheelchair propulsion and it is difficult to quantify co-contraction using these methods. However, there has been no report of co-contraction in the upper extremity during the majority of the propulsion cycle.

Acknowledgements

This work was supported by the National Health Research Institute grant NHRI-EX90-9019EL and National Science Council grant NSC89-2614-E-242-001, TAIWAN.

References

Asato, K.T., Cooper, R.A., Robertson, R.N., Ster, J.F., 1993. Smartwheels: development and testing of a system for measuring manual wheelchair propulsion dynamics. IEEE Trans. Biomed. Eng. 40, 1320–1324.

Bednarczyk, J.H., Sanderson, D.J., 1995. Limitations of kinematics in the assessment of wheelchair propulsion in adults and children with spinal cord injury. Phys. Ther. 75, 281–289.

Boninger, M.L., Cooper, R.A., Robertson, R.N., Shimada, S.D., 1997. 3-dimensional pushrim forces during 2 speeds of wheelchair propulsion. Am. J. Phys. Med. Rehabil. 76, 420–426.

Boninger, M.L., Souza, A.L., Cooper, R.A., Fitzgerald, S.G., Koontz, A.M., Fay, B.T., 2002. Propulsion patterns and pushrim biomechanics in manual wheelchair propulsion. Arch. Phys. Med. Rehabil. 83, 718–723.

Burdett, R.G., Skrinar, G.S., Simon, S.R., 1983. Comparison of mechanical work and metabolic energy consumption during normal gait. J. Orthop. Res. 1, 63–72.

Cooper, R.A., Robertson, R.N., Vansickle, D.P., Boninger, M.L., Shimada, S.D., 1997. Methods for determining three-dimensional wheelchair pushrim forces and moments: a technical note. J. Rehabil. Res. Dev. 34, 162–170.

Dallmeijer, A.J., Van Der Woude, L.H., Veeger, H.E., Hollander, A.P., 1998. Effectiveness of force application in manual wheelchair

propulsion in persons with spinal cord injuries. Am. J. Phys. Med. Rehabil. 77, 213–221.

Davis, J.L., Growney, E.S., Johnson, M.E., Iuliano, B.A., An, K.N., 1998. Three-dimensional kinematics of the shoulder complex during wheelchair propulsion: a technical report. J. Rehabil. Res. Dev. 35, 61–72.

De Groot, S., Veeger, H.E.J., Hollander, A.P., Van Der Woude, L.H.V., 2002. Consequence of feedback-based learning of an effective hand rim wheelchair force production on mechanical efficiency. Clin. Biomech. 17, 219–226.

De Groot, S., Veeger, H.E., Hollander, A.P., Van Der Woude, L.H., 2003. Adaptations in physiology and propulsion techniques during the initial phase of learning manual wheelchair propulsion. Am. J. Phys. Med. Rehabil. 82, 504–510.

Frost, G., Dowling, J., Baror, O., Dyson, K., 1997. Ability of mechanical power estimations to explain differences in metabolic cost of walking and running among children. Gait Posture 5, 120–127.

Gordon, D., Robertson, E., Winter, D.A., 1980. Mechanical energy generation, absorption and transfer amongst segments during walking. J. Biomech. 13, 845–854.

Guo, L.Y., Su, F.C., Wu, H.W., An, K.N., 2003. Mechanical energy and power flow of the upper extremity in manual wheelchair propulsion. Clin. Biomech. 18, 106–114.

Hughes, C.J., Weimar, W.H., Sheth, P.N., Brubaker, C.E., 1992. Biomechanics of wheelchair propulsion as a function of seat position and user-to-chair interface. Arch. Phys. Med. Rehabil. 73, 263–269.

Masse, L.C., Lamontagne, M., O'riain, M.D., 1992. Biomechanical analysis of wheelchair propulsion for various seating positions. J. Rehabil. Res. Dev. 29, 12–28.

Morrow, D.A., Guo, L.Y., Zhao, K.D., Su, F.C., An, K.N., 2003. A 2-d model of wheelchair propulsion. Disabil. Rehabil. 25, 192–196.

Mulroy, S.J., Farrokhi, S., Newsam, C.J., Perry, J., 2004. Effects of spinal cord injury level on the activity of shoulder muscles during wheelchair propulsion: an electromyographic study. Arch. Phys. Med. Rehabil. 85, 925–934.

Robertson, R.N., Boninger, M.L., Cooper, R.A., Shimada, S.D., 1996. Pushrim forces and joint kinetics during wheelchair propulsion. Arch. Phys. Med. Rehabil. 77, 856–864.

Rodgers, M.M., Tummarakota, S., Lieh, J., 1998. Three-dimensional dynamic analysis of wheelchair propulsion. J. App. Biomech. 14, 80–92.

Rozendaal, L.A., Veeger, H.E.J., Van Der Woude, L.H.V., 2003. The push force pattern in manual wheelchair propulsion as a balance between cost and effect. J. Biomech. 36, 239–247.

Rudins, A., Laskowski, E.R., Growney, E.S., Cahalan, T.D., An, K.N., 1997. Kinematics of the elbow during wheelchair propulsion: a comparison of two wheelchairs and two stroking techniques. Arch. Phys. Med. Rehabil. 78, 1204–1210.

Ruggles, D.L., Cahalan, T., An, K.N., 1994. Biomechanics of wheelchair propulsion by able-bodied subjects. Arch. Phys. Med. Rehabil. 75, 540–544.

Sabick, M.B., Kotajarvi, B.R., An, K.-N., 2004. A new method to quantify demand on the upper extremity during manual wheelchair propulsion. Arch. Phys. Med. Rehabil. 85, 1151–1159.

Su, F.C., Lin, L.T., Wu, H.W., Chou, Y.L., Westreich, A., An, K.N., 1993. Three-dimensional dynamic analysis of wheelchair propulsion. Chin. J. Med. Biol. Eng. 13, 329–342.

Unnithan, V.B., Dowling, J.J., Frost, G., Baror, O., 1999. Role of mechanical power estimates in the o-2 cost of walking in children with cerebral-palsy. Med. Sci. Sports Exerc. 31, 1703–1708.

Van Der Helm, F.C.T., Veeger, H.E.J., 1999. Shoulder modelling in rehabilitation: the power balance during wheelchair propulsion. In: Van Der Woude, L.H.V., Hopman, M.T.E., Van Kememade, C.H. (Eds.), Biomedical Aspects of Manual Wheelchair Propulsion: The State of the Art ii. IOS Press, Amsterdam, Netherland, pp. 96–103.

Van Der Linden, M.L., Valent, L., Veeger, H.E., Van Der Woude, L.H., 1996. The effect of wheelchair handrim tube diameter on propulsion efficiency and force application (tube diameter and efficiency in wheelchairs). IEEE Trans. Rehabil. Eng. 4, 123–132.

Van Der Woude, L.H., Veeger, D.J., Rozendal, R.H., Sargeant, T.J., 1989. Seat height in handrim wheelchair propulsion. J. Rehabil. Res. Dev. 26, 31–50.

Van Der Woude, L.H., Veeger, H.E., Rozendal, R.H., Van Ingen Schenau, G.J., Rooth, F., Van Nierop, P., 1988. Wheelchair racing: effects of rim diameter and speed on physiology and technique. Med. Sci. Sports Exerc. 20, 492–500.

Van Drongelen, S., Van Der Woude, L.H., Janssen, T.W., Angenot, E.L., Chadwick, E.K., Veeger, D.H., 2005. Mechanical load on the upper extremity during wheelchair activities. Arch. Phys. Med. Rehabil. 86, 1214–1220.

Veeger, H.E.J., Van Der Woude, L.H.V., 1991. Load on the upper extremity in manual wheelchair propulsion. J. Electromyogr. Kinesiol. 1, 270–280.

Veeger, D., Van Der Woude, L.H., Rozendal, R.H., 1989. The effect of rear wheel camber in manual wheelchair propulsion. J. Rehabil. Res. Dev. 26, 37–46.

Veeger, H.E., Van Der Woude, L.H., Rozendal, R.H., 1991. Within-cycle characteristics of the wheelchair push in sprinting on a wheelchair ergometer. Med. Sci. Sports Exerc 23, 264–271.

Veeger, H.E., Lute, E.M., Roeleveld, K., Van Der Woude, L.H., 1992a. Differences in performance between trained and untrained subjects during a 30-s sprint test in a wheelchair ergometer. Eur. J. Appl. Physiol. 64, 158–164.

Veeger, H.E., Van Der Woude, L.H., Rozendal, R.H., 1992b. Effect of handrim velocity on mechanical efficiency in wheelchair propulsion. Med. Sci. Sports Exerc 24, 100–107.

Wei, S.H., Huang, S.L., Jiang, C.J., Chiu, J.C., 2003. Wrist kinematic characterization of wheelchair propulsion in various seating positions: Implication to wrist pain. Clin. Biomech. 18, S46–S52.

Winter, D.A., 1994. Biomechanics and Motor Control of Human Movement. John-Wiley & Sons, New York.

Wu, H.W., Berglund, L.J., Su, F.C., Yu, B., Westreich, A., Kim, K.J., An, K.N., 1998. An instrumented wheel for kinetic analysis of wheelchair propulsion. J. Biomech. Eng. 120, 533–535.